Journal of Power Sources 195 (2010) 5144–5149

Contents lists available at ScienceDirect

Journal of Power Sources

journal homepage: www.elsevier.com/locate/jpowsour

Effect of length of anodized TiO_2 tubes on photoreactivity: Photocurrent, Cr(VI) reduction and H_2 evolution

Minsung Park[a], Ahyoung Heo[a], Eunjung Shim[b], Jaekyung Yoon[b], Hansung Kim[a], Hyunku Joo[b,*]

[a] Dept. of Chemical and Biomolecular Engineering, Yonsei University, 262 Seongsanno, Seodaemun-gu, Seoul 120-749, Republic of Korea
[b] Hydrogen Energy Research Center, New and Renewable Energy Research Division, Korea Institute of Energy Research, 71-2 Jang-dong, Yuseong-gu, Daejeon 305-343, Republic of Korea

ARTICLE INFO

Article history:
Received 11 December 2009
Received in revised form 8 February 2010
Accepted 15 February 2010
Available online 1 March 2010

Keywords:
Anodization
Photoanode
Enzymatic cathode
Photocatalysis
Immobilized titania

ABSTRACT

Anodized tubular TiO_2 electrodes (ATTEs) are prepared using an organic additive consisting of either (i) ethylene glycol (EG) or (ii) glycerol (Gly) to make various photoanodes with different length of TiO_2 tubes and thereby to investigate the effect of their length on the photo-driven activity for hydrogen evolution and Cr(VI) reduction, as well as on the photocurrent. The ATTEs with EG have longer TiO_2 tubes (3.42–15.6 μm) than those with Gly (0.26–1.95, 6.82 μm). The former samples exhibit higher photocurrent densities (22.8–32.8 mA cm^{-2}) than the latter (8.0–19.4, 20.3 mA cm^{-2}). The latter samples (tube length of less than 7 μm) clearly exhibit a change of the rate-determining step from electron migration to photohole capture as the scanned applied bias increases, since the photocurrent shows a plateau for tube lengths above 2 μm. Meanwhile, the samples with EG remain in the electron migration step up to a tube length of 16 μm and is due to the difference of the morphology, crystal phase and crystallinity. This favourable characteristic is also applied to and well matched with the results from the reactions of Cr(VI) reduction and hydrogen evolution (up to ca. 250 μmol h^{-1}).

1. Introduction

The conversion of harmful chemicals into nontoxic substances by photocatalysis has been of interest since the early 1970s when Honda and Fujishima first performed their pioneering work using solar light and UV-absorbing TiO_2 [1]. At the same time, there is increasing interest in the use of hydrogen, which has the potential to supplement and ultimately replace fossil fuels for the production of energy and is favoured in terms of reducing the emission of greenhouse gases. Immobilized photocatalysts on conducting substrates have been used as both the key part of light-driven purification systems and the photoanode of photoelectrochemical (PEC) systems, which are non-polluting, waste free, sustainable processes. The overall efficiency of the two systems is determined by a combination of factors, such as imperfections in the crystalline structure, bulk and surface properties, ease of preparation and resistance to corrosion of the photocatalytic material in electrolytes [2]. In general, the photocatalytic process has been criticized as being uneconomical compared with other methods for hydrogen production, due to its inherently low efficiency and resulting high overall energy cost [3]. Hence, to improve the conversion efficiency obtained with solar energy, it is essential to design an energetically coordinated, stably operated, and economically feasible photocatalyst-immobilized matrix. Concerning this issue, many recent publications and reviews have addressed the photoelectrochemical production of hydrogen [4,5], semiconductor particulate systems [3], TiO_2 photocatalysts [6] and other material-related issues [4,7]. Compared with other photocatalytic materials, TiO_2 is much more promising and its functional properties for solar hydrogen production have been thoroughly summarized in a previous report [8].

Over the past few decades, photoanodes covered with TiO_2-based films have been prepared using techniques such as anodization [9–14] and sputtering [15]. Meanwhile, TiO_2 nanotube arrays on Ti foil have attracted particular interest as light-sensitizing material for photocatalytic purification, photoanodes' and cathodic substrates for the enzymatic production of hydrogen driven by light [16–20]. Since the widespread use of TiO_2 is inhibited by its limited response to UV light with wavelengths of less than 387 nm, further research to extend its photoresponse to the visible-light region must be conducted through approaches such as the co-doping of F and P or B into the TiO_2 matrix [21,22]. The other issue is the optimum increase in the amount of the photocatalyst with regard to the issues of electron migration and photohole capture. For the latter issue, this study presents the effect of the tube length of the anodized Ti foils with an organic additive in the electrolyte on the photo-reactivity such as the photocurrent, Cr(VI) reduction and hydrogen evolution.

* Corresponding author. Tel.: +82 42 860 3563; fax: +82 42 860 3134.
E-mail address: hkjoo@kier.re.kr (H. Joo).

0378-7753/$ – see front matter © 2010 Elsevier B.V. All rights reserved.
doi:10.1016/j.jpowsour.2010.02.065

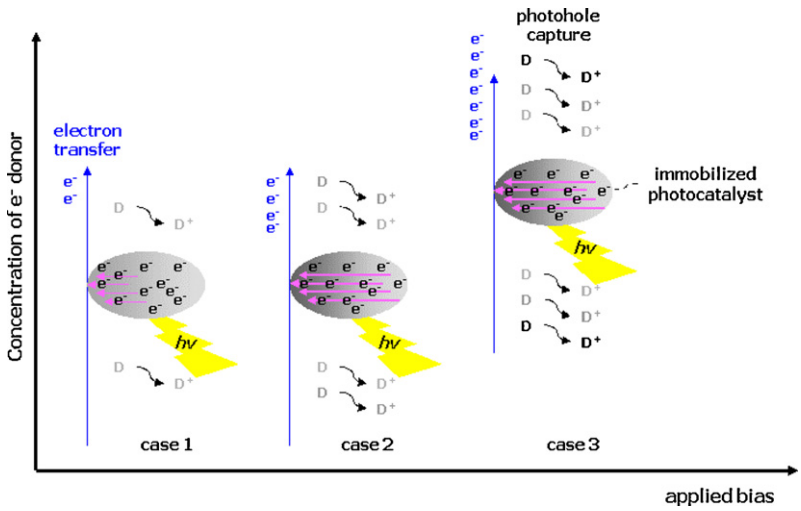

Fig. 1. Schematic representation of amount of transferred electrons with respect to applied bias and concentration of electrolyte.

2. Experimental

2.1. Materials and sample preparation

Titanium foil (Ti, 99.6 wt.% purity, thickness 0.25 mm, Goodfellow, England) was cut into pieces (2 cm × 4 cm) and subjected to potentiostatic anodization in a two-electrode electrochemical cell (100 ml of an electrolyte) that was connected to a d.c. power supply and employed a platinum counter electrode with magnetic agitation. The samples were then annealed in an oxygen or air atmosphere (400 ml min^{-1}) at 450 or 650 °C for 2 h. The electrolytes were (i) 0.3 M NH_4F (99.99 vol.%, Sigma–Aldrich) + 2 vol.% H_2O + ethylene glycol (EG; 99.8 vol.%, Sigma–Aldrich), (ii) 0.15 M NH_4F (99.99 vol.%, Sigma–Aldrich) + 3 vol.% H_2O + glycerol (Gly; 99.5 vol.%, Sigma–Aldrich) and, for comparison and the immobilization of the enzyme, 0.5 vol.% hydrofluoric (HF) acid at 5 °C (48–51 vol.%, DC Chemical) was also used. The resulting electrode is called an 'anodized tubular TiO_2 electrode' or 'ATTE'. A detailed explanation of the role of each component of the anodizing solution is available in the literature [9–13].

The area of the illuminated working electrode (prepared ATTE) and the cathode for the immobilization of hydrogenase was 1 cm × 1 cm (20 V at 5 °C for 45 min, then heat-treated at 650 °C under an O_2 flow rate of 400 ml min^{-1}). Potassium hydroxide solution (1.0 M) was prepared from KOH pellets (99.99 wt.%, Sigma–Aldrich) and used as the electrolyte in both compartments for hydrogen evolution. Purified hydrogenase (from *Pyrococcus furiosus*, '*Pfu*' hereafter) was supplied by the University of Georgia and this enzyme is known to be remarkably resistant to inactivation by heat and chemical reagents [23]. Details concerning the immobilization of the enzyme are described in the literature [17–20]. With the previously used [17–20] aryl azide crosslinking reagent, Sulfo-SANPAH (spacer arm 18.2 Å, PIERCE Biotechnology, USA) and Sulfo-SDA (spacer arm 3.9 Å, PIERCE Biotechnology, USA) were used to investigate the effect of the length of the spacer arm of the crosslinker on the electron transfer capability in the cathode part of the light-sensitized, enzymatic system for hydrogen production.

2.2. Apparatus and analysis

The experiments for Cr(VI) reduction were conducted in a photocatalytic reactor. The volume of the reactor was 200 ml and it contained an aqueous solution in which the initial concentration of Cr(VI) and pH were adjusted. Potassium dichromate ($K_2Cr_2O_7$, 99.5 wt.%, Oriental Chemical Industries, Korea) was used to make the initial Cr(VI) solution. It is known [16] that the surface charges of all ATTEs are positive at pH 3 and become more negative with increasing pH and that Cr(VI) ions ($Cr_2O_7^{2-}$) are the predominant species at medium-to-low pH values. Therefore, the experiments for Cr(VI) reduction were conducted at pH = 3 with HCl. The outside of the reactor was water-jacketted to maintain a constant reaction temperature. Prior to reaction, the immobilized nanotubular TiO_2 was fixed in the middle of the aqueous solution with UV light.

Cyclic voltammetry for measurement of the photocurrent was applied to evaluate the electrochemical behaviour of the ATTEs using a potentiostat (G300 with a PHE200 software, GAMRY Instruments Electrochemistry, PA, USA) with a platinum mesh electrode as the counter electrode and Ag|AgCl (saturated in 3.0 M KCl) as the reference electrode.

For hydrogen evolution, the experiments were conducted in a two-compartment reactor, i.e., anodic and cathodic parts separated by a nanofiltration (NF) membrane and a solar cell. Detailed description of the NF membrane and solar panel has been reported previously [17–20]. Prior to reaction, the mixture was de-aerated with argon gas for 30 min to remove the oxygen in the water and headspace, unless otherwise stated.

The light source used for the hydrogen evolution reactions was a 1000 W xenon lamp (Oriel, USA), which was filtered through a 10-cm IR water filter. The irradiated light intensity was ca. 74 ± 3.4 mW cm^{-2} (at 350–450 nm with a portable radiometer with UM-10 and UM-400, from Minolta Co., Japan). The hydrogen produced was analyzed with a gas chromatograph and a thermal conductivity detector (TCD at 260 °C, oven at 40 °C). The column used in the system was a molecular sieve 5A (Supelco, USA).

The crystal phase and size were determined by X-ray diffraction (XRD, Miniflex, Rigaku, Japan; k = 0.89, lambda = 0.15418 for Cu Kα X-ray, 30 kV, 15 mA) and the concentration of Cr(VI) was analyzed colorimetrically by means of UV/Vis spectroscopy (SCINCO, S-3150, Korea). In this analysis, the 1,5-diphenylcarbazide method was used [24,25]. The structure and morphological characterizations were conducted with a scanning election microscope (SEM, Hitachi S-4700, Japan). A contact angle analyzer (Phoeni X150, SEO, Korea) was used to measure the contact angle of the selected ATTEs by the sessile drop method and was based on the angle between the water droplet and the ATTE surface.

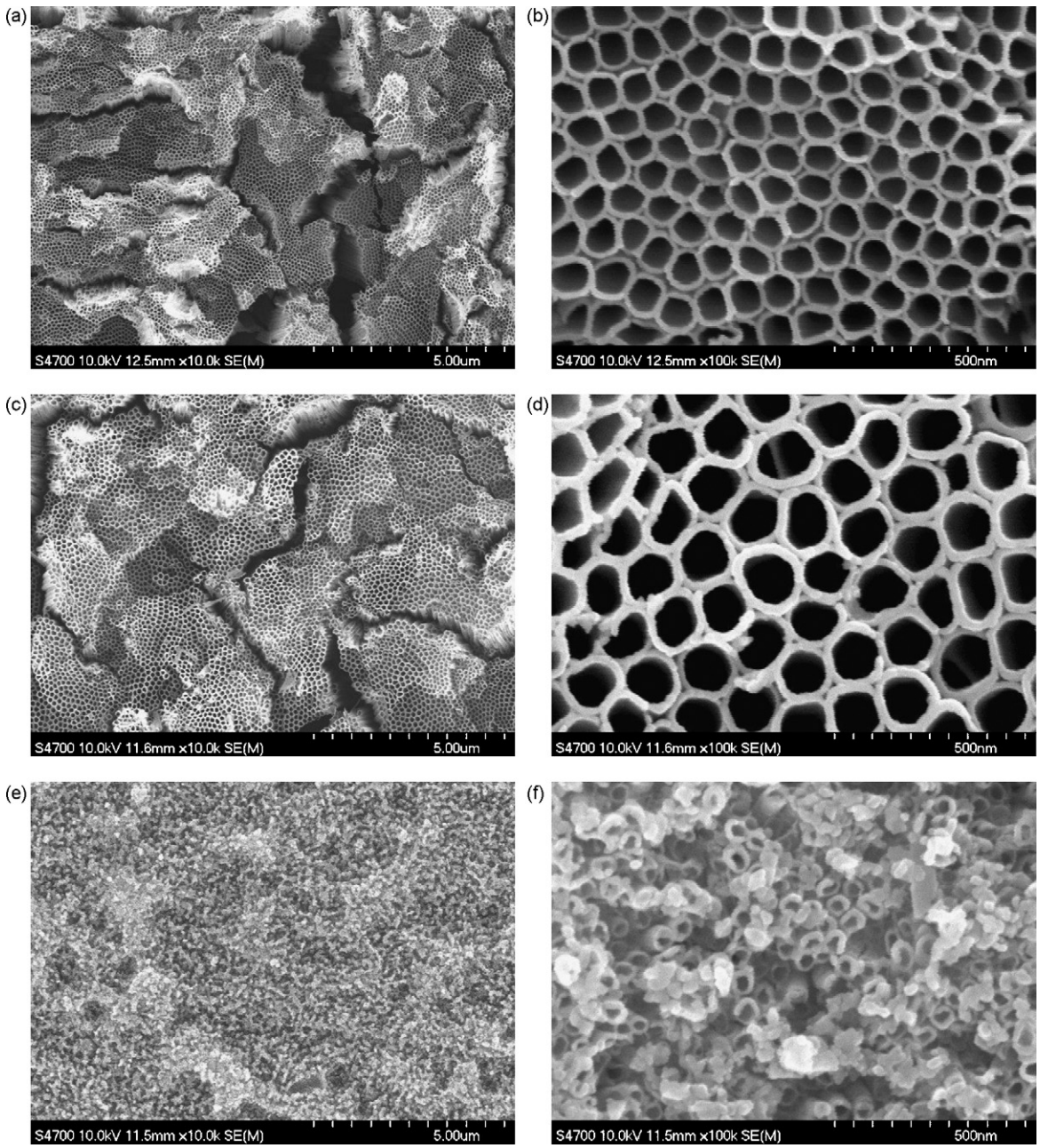

Fig. 2. Scanning electron micrographs of the selected samples with low (left) and high (right) magnification: (a and b) anodized at 55 V for 3 h; (c and d) anodized at 0.1 A for 3 h in 0.3 M NH_4F + 2 vol.% H_2O + EG – treated at 450 °C for 2 h in O_2 400 ml min^{-1}, (e and f) anodized at 20 V for 24 h in 0.15 M NH_4F + 3 vol.% H_2O + Gly – treated at 450 °C for 2 h in air 400 ml min^{-1}.

3. Results and discussion

The colour of the as-anodized samples with 'electrolyte i' is dark green and changes into blue after heat-treatment, while that of the as-anodized samples with 'electrolyte ii' is bright green and becomes bright blue after heat-treatment. There is no noticeable hump in the region of 400–540 nm in the UV–Vis spectra of the samples, as reported by Varghese et al. [26] in which heat-treatment at 450 °C under nitrogen is performed [26]. This discrepancy may arise from the environment used for the heat-treatment. Further detailed study such as the action spectrum is required to understand the visible light sensitization.

While the morphology of the ATTE varies noticeably according to the electrolyte, applied voltage and bath temperature [17–20], in the present study, the length of the TiO_2 tubes on the anodized Ti foil is highly correlated with their photoelectrochemical activity. In fact, an increased in the length of the tubes might enhance the rate of Cr(VI) reduction and photocurrent density, due to an increase in the amount of photocatalytic materials, in other words, their large surface area and more excited electrons (Fig. 1). As shown in Fig. 1, when either the applied bias or the amount of photoreactive material is low, the number of electrons transportable to the outside of the immobilized particles is also limited. Hence, the rate-determining step is electron migration within the semiconducting material (case 1 in Fig. 1). Increasing the bias can help the electrons to move to some extent, and there by result in an increase in the photocurrent (case 2 in Fig. 1). Meanwhile, when the applied bias is sufficiently high to pull all of the excited electrons, the concentration of electron donors (or photohole capture) can be the rate-determining step (case 3 in Fig. 1). Jiang et al. [27]

have also studied the relationship between the photocatalytic oxidation of different organic compounds and the applied bias using the photoelectrochemical method.

Selected SEM images (surface view) of the prepared ATTEs are given in Fig. 2. The first set of images (a and b) correspond to the sample prepared in 'electrolyte i' with a fixed bias (55 V) for 3 h, the second (c and d) in 'electrolyte i' with a fixed current (0.1 A) for 3 h, and the third (e and f) in 'electrolyte ii' with 20 V for 24 h (treated at 450 °C). The TiO_2 nanotubular arrays are vertically oriented and more compact and straight in the samples with EG (a, b and c, d) than those in the samples with Gly (e and f). Anodization for 0.5 and 1 h in 'electrolyte i' appears to be insufficient to allow the nanotubes to develop fully (data not shown). Using a higher heat-treatment temperature (650 °C) for the samples with Gly caused the top of the nanotubes to crumble and stick together, and this problem became more severe when a longer anodization time is employed. It is considered that with the application of an external bias, more electrons can be supported by the greater amount of hole capture which is provided by water oxidation in this study. The hole diffusion length in titania is ca. 10 nm, while the electron diffusion length is ca. 10 μm [26]. Therefore, one-dimensional TiO_2 nanotubes with half the wall thickness of 10 nm are essential for charge generation and transport. The samples with EG show less than 10 nm of half the wall thickness and very straight tubes standing on the Ti foil.

The X-ray diffraction patterns were recorded and are shown in Fig. 3. All of the as-anodized samples are found to be amorphous, while heat-treatment in dry O_2 leads to the dominant formation of the anatase phase at 450 °C, and rutile phase appears at 650 °C when EG is added to the anodizing electrolyte (electrolyte i). Interestingly, when Gly is added (electrolyte ii), a longer anodization time facilitates the creation of anatase crystallines and heat-treatment at a higher temperature (650 °C) with the same anodization time causes the rutile crystallines to be prevalent. This does not happen in 'electrolyte i', but anodization with HF electrolyte shows the same rutile phase growth after heat-treatment at 550 °C and above. Generally, the samples with EG show a higher degree of crystallinity that those with Gly.

Cyclic voltammetry in 1.0 M KOH at 25 °C was applied to evaluate the photocurrent generated from the prepared ATTE samples. The immobilization of TiO_2 with the formation of TiO_2 nanotubes standing on the Ti foil by anodization makes it possible to apply the electrochemistry technique to analyze the characteristics, as well as providing better stability and an improved geometric structure for the reaction. The generated photocurrents are shown in Fig. 4. The samples with EG, which have longer TiO_2 tubes, create high photocurrents that range from 22.8 to 32.8 mA cm^{-2}, while the samples with Gly, which have shorter tubes, produce photocurrent from 8.0 to 19.4 (20.3 max.) mA cm^{-2}. The latter samples (tube length of less than 7 μm) clearly exhibit a change in the rate-determining step from electron migration to photohole capture as the scanned applied bias increases, since the photocurrent shows a plateau at tube lengths of 2 μm and above. Meanwhile, the samples with EG remain in the electron migration step up to a tube length of 16 μm. This is due to their different morphology, crystal phase and crystallinity. Samples with a more compact structure, less rutile phase and higher crystallinity facilitate the transport of electrons activated by the incident light to the counter electrode. From the SEM images and XRD patterns, therefore, it can be inferred that the higher photocurrents from the samples with EG are well matched. Heat treatment at 650 °C has a more detrimental effect on the photocurrent of the samples with EG than on those with Gly (large circles in Fig. 4).

The photocatalytic reduction of Cr(VI) with the ATTEs in 'electrolyte i' was performed at different initial concentrations that ranged from 2 to 10 ppm and pH = 3. At a low initial concentration,

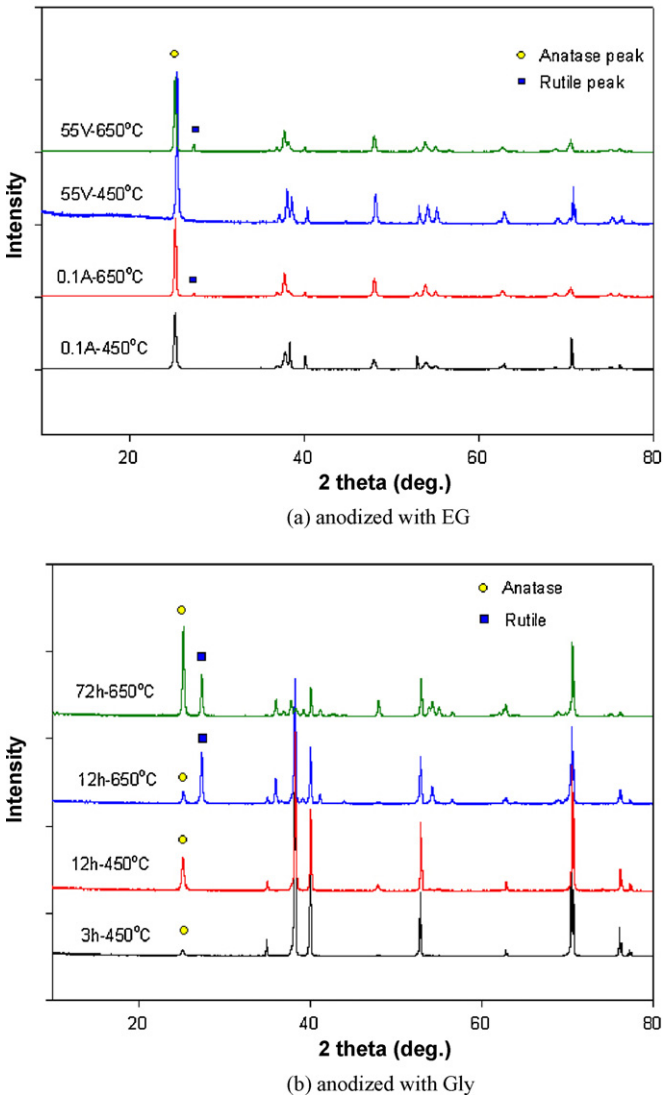

Fig. 3. XRD patterns of selected samples: (a) anodized with EG; (b) anodized with Gly.

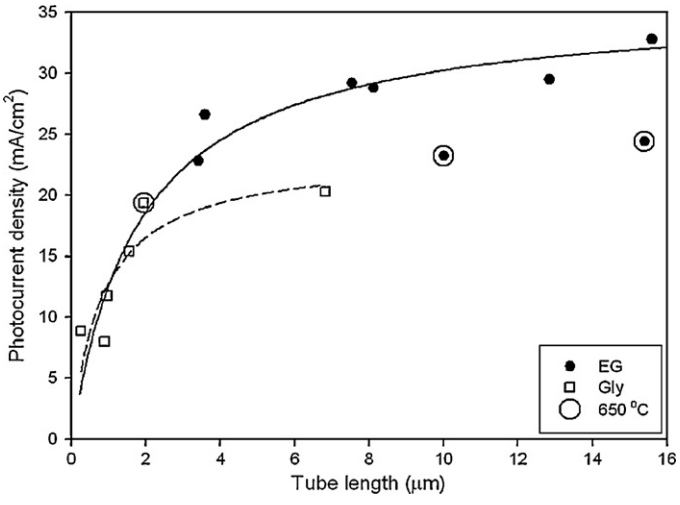

Fig. 4. Plot of photocurrent vs. length of TiO_2 tubes on anodized samples.

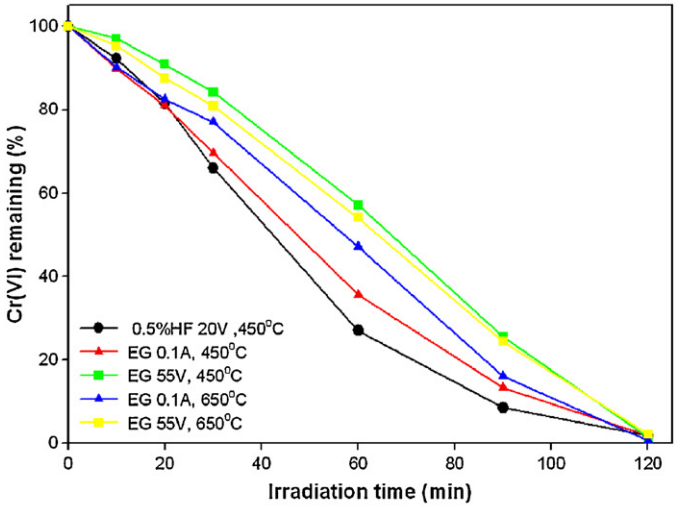

(a) Initial concentration of Cr(VI)=2 ppm at pH=3 with 1kW Xe lamp

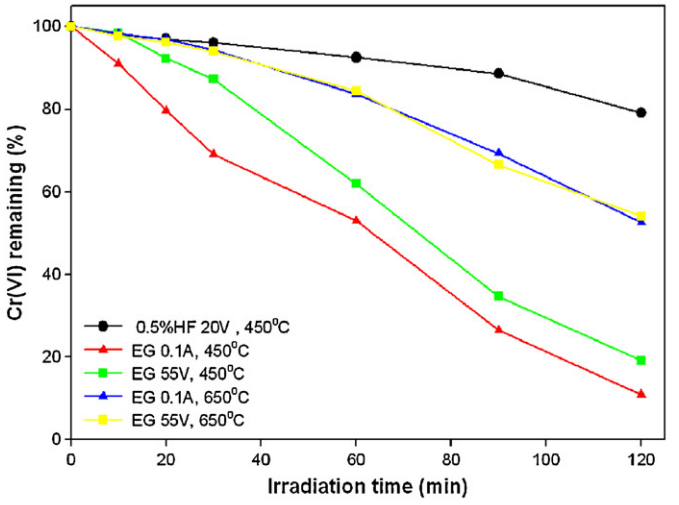

(b) Initial concentration of Cr(VI)=5 ppm at pH=3 with 1kW Xe lamp

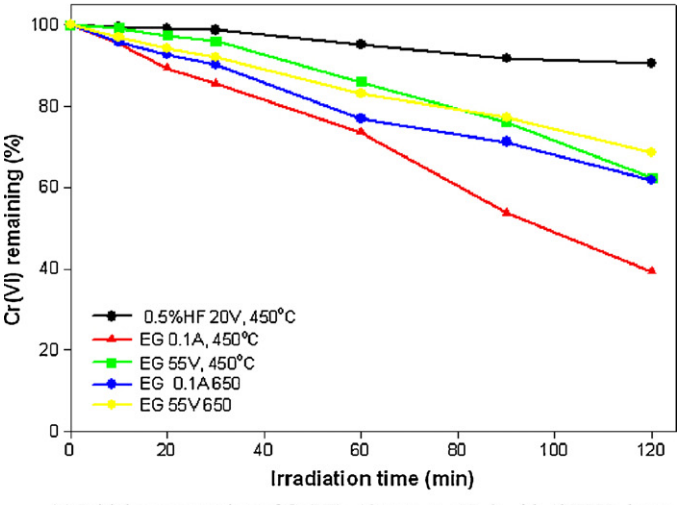

(c) Initial concentration of Cr(VI)=10 ppm at pH=3 with 1kW Xe lamp

Fig. 5. Effect of anodized conditions on Cr(VI) reduction at pH = 3: (a) initial concentration = 2 ppm; (b) initial concentration = 5 ppm; (c) initial concentration = 10 ppm. '0.5 wt.% HF 20 V' means anodized at 20 V for 45 min at bath i.e., temp. 5 °C in 0.5 wt.% HF and then treated 450 °C for 2 h under ambient gas flow O_2 400 ml min^{-1}.

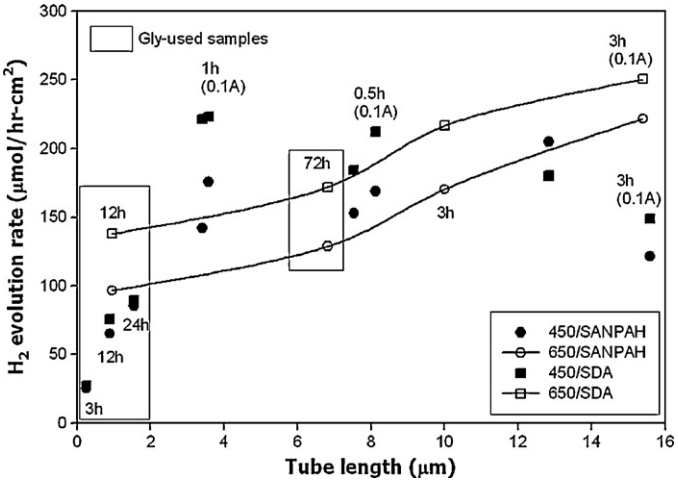

Fig. 6. Hydrogen evolution rate vs. length of TiO_2 tubes on anodized samples with different spacer arms of crosslinker and heat-treatment temperatures.

longer TiO_2 tubes are not necessary to reduce Cr(VI) and shorter tubes (ca. 0.6 μm) are sufficient and even more active than the longer ones (Fig. 5(a)). This may be caused by the fact that the penetration of the irradiated photons into the inside and bottom of the longer tubes, where the Cr(VI) ions can be adsorbed, is hindered. At a higher concentration, a large surface area is essential and Cr(VI) ions are adsorbed over the entire inner surface of the longer tubes. As shown in Fig. 5(b) and (c), the samples prepared with EG at a fixed current (0.1 A) and heat treated at 450 °C show the best reactivity. The results obtained with the samples with Gly also demonstrate the same tendency, wherein the samples with a higher photocurrent (20 V, 72 h-450 °C) have better activity for Cr(VI) reduction and, indeed, much better activity that the samples with HF (short tubes).

The prepared samples were also used as anodes in a light-sensitized enzymatic system with the same enzyme-immobilized cathode. Without any applied bias or a co-catalyst, titania cannot effectively reduce water to produce hydrogen because the position of the flat-band potential is close to the reduction potential of water [26]. In the present study, an examination is made of the effect of the length of the TiO_2 tubes and the length of the spacer arm of the crosslinker used to connect the enzymes to the surface of the TiO_2 tubes. The results are summarized in Fig. 6. In general the reactions with longer tubes at the photoanode evolve more hydrogen, as expected. In particular, for the samples heat-treated at 450 °C (filled symbols), the amount of hydrogen evolved increases with increasing tube length in a decelerating manner. This trend appears to be linear up to a tube length of 4 μm, exhibits a square-root tendency (~ca. 10 μm), and then decreases. Meanwhile, for samples heat-treated at 650 °C (open symbols), the amount of hydrogen produced increases linearly with increasing tube length within the range investigated. The higher photocurrent obtained with the longer tubes means that more electrons move to the cathode, which is essential to reduce the protons to hydrogen molecules. Hence, a higher photocurrent leads to more hydrogen being produced, provided there are no other defects in the system. The photoelectrochemical behaviour is governed by Faraday's law. As far as the crosslinkers are concerned, a shorter spacer arm (3.9 Å) in the crosslinker at the cathodic part makes the transport length of the electrons shorter than that with a longer spacer arm (18.2 Å), which lessens the probability of charge recombination. This seems to be the reason why the samples with SDA (squares in Fig. 6) clearly evolve more hydrogen than the samples with SANPAH (circles in Fig. 6).

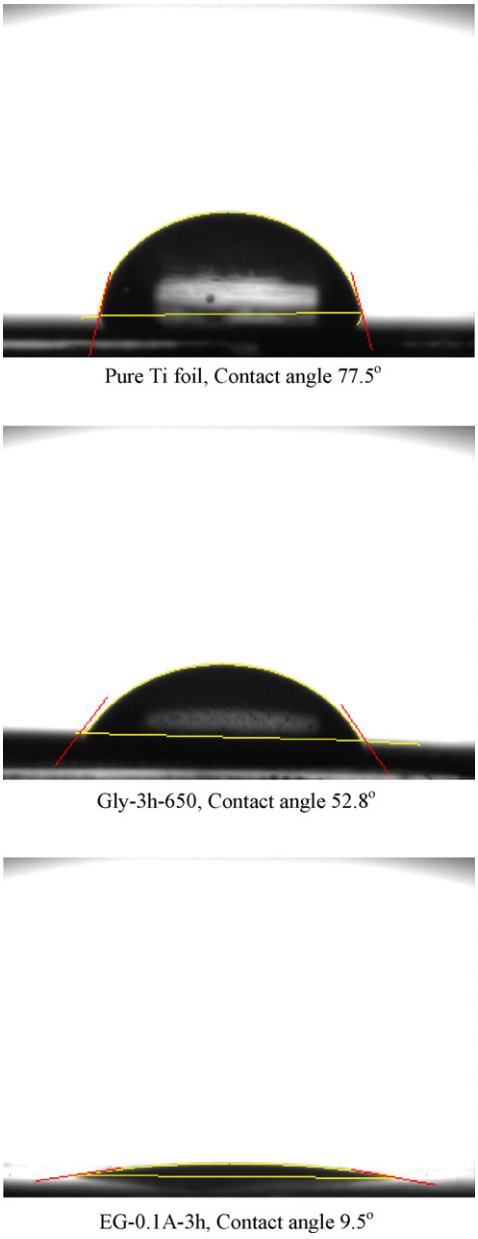

Fig. 7. Comparison of contact angles for selected samples: (a) pure Ti foil; (b) sample anodized with Gly; (c) sample anodized with EG.

The contact angles of the samples were measured and the results are given in Fig. 7. The samples with longer TiO_2 tubes have lower contact angles that range from 77.5° for pure Ti foil to 9.5° for the sample anodized with EG at a fixed current. This result also suggests the possible application of anodized materials with longer tubes in outdoor building materials for self-cleaning.

4. Conclusions

Anodized tubular TiO_2 electrodes (ATTEs) are prepared using an organic additive to investigate the effect of the length of the TiO_2 tubes on the photo-driven activity for the reactions of hydrogen evolution and Cr(VI) reduction, as well as the photocurrent. ATTEs with longer TiO_2 tubes generally yield a higher photocurrent, higher activity for Cr(VI) reduction, and more hydrogen evolution. These results are attributed to the increased amount of TiO_2 (namely, the surface area) with a well-defined structure (vertically standing nanotubes) and a crystalline phase, which facilitate the transport of the photo-generated electrons.

Acknowledgement

This research was performed for the Hydrogen Energy R&D Center, one of the 21st Century Frontier R&D Programs, funded by the Ministry of Education, Science and Technology of Korea.

References

[1] A. Fujishima, K. Honda, Nature 238 (1972) 37–38.
[2] V.M. Aroutiounian, V.M. Arakelyan, G.E. Shahnazaryan, Sol. Energy 78 (5) (2005) 581–592.
[3] M. Ashokkumar, Int. J. Hydrogen Energy 23 (1998) 427.
[4] T. Bak, J. Nowotny, M. Rekas, C.C. Sorrell, Int. J. Hydrogen Energy 27 (2002) 991–1022.
[5] S. Malato, J. Blanco, A. Vidal, C. Richter, Appl. Catal. B 37 (2002) 1–15.
[6] M. Ni, M.K.H. Leung, D.Y.C. Leung, K. Sumathy, Renew. Sust. Energy Rev. 11 (2007) 401.
[7] T. Bak, J. Nowotny, M. Rekas, C.C. Sorrell, Int. J. Hydrogen Energy 27 (2002) 19.
[8] J. Nowotny, T. Bak, M.K. Nowotny, L.R. Sheppard, Int. J. Hydrogen Energy 32 (14) (2007) 2609.
[9] D. Gong, C.A. Grimes, O.K. Varghese, W. Hu, R.S. Singh, Z. Chen, E.C. Dickey, J. Mater. Res. 16 (2001) 3331.
[10] O.K. Varghese, D. Gong, M. Paulose, C.A. Grimes, E.C. Dickey, J. Mater. Res. 18 (2003) 156.
[11] G.K. Mor, O.K. Vargheese, M. Paulose, N. Mukherjee, C.A. Grimes, J. Mater. Res. 18 (2003) 2588.
[12] G.K. Mor, K. Shankar, M. Paulose, O.K. Vargheese, C.A. Grimes, Nano Lett. 5 (2005) 191.
[13] M. Paulose, G.K. Mor, O.K. Vargheese, K. Shankar, C.A. Grimes, J. Photochem. Photobiol. A: Chem. 178 (2006) 8.
[14] K.S. Raja, V.K. Mahajan, M. Misra, J. Power Sources 159 (2006) 1258.
[15] M. Kitano, M. Takeuchi, M. Matsuoka, J.M. Thomas, M. Anpo, Catal. Today 120 (2007) 133.
[16] J. Yoon, E. Shim, S. Bae, H. Joo, J. Hazard. Mater. 161 (2009) 1069–1074.
[17] S. Bae, E. Shim, J. Yoon, H. Joo, Sol. Energy Mater. Sol. Cells 92 (2008) 402–409.
[18] S. Bae, J. Kang, E. Shim, J. Yoon, H. Joo, J. Power Sources 179 (2) (2008) 863–869.
[19] S. Bae, E. Shim, J. Yoon, H. Joo, J. Power Sources 185 (2008) 439–444.
[20] E. Shim, Y. Park, S. Bae, J. Yoon, H. Joo, Int. J. Hydrogen Energy 33 (2008) 5193.
[21] X. Chen, X. Zhang, Y. Su, L. Lei, Appl. Surf. Sci. 254 (2008) 6693–6696.
[22] Y. Su, S. Han, X. Zhang, X. Chen, L. Lei, Mater. Chem. Phys. 110 (2008) 239.
[23] F.O. Bryant, M.W.W. Adams, J. Biol. Chem. 264 (9) (1989) 5070.
[24] V. Osokov, B. Kebbekus, D. Chesbro, Anal. Lett. 29 (10) (1996) 1829–1850.
[25] X. Wang, S.O. Pehkonen, A.K. Ray, Ind. Eng. Chem. Res. 43 (2004) 1665–1672.
[26] O.K. Varghese, M. Paulose, T.J. LaTempa, C.A. Grimes, Nano Lett. 9 (2) (2009) 731–737.
[27] D. Jiang, H. Zhao, S. Zhang, R. John, J. Photochem. Photobiol. A: Chem. 177 (2006) 253–260.